Enhancement of the anomalous Nernst effect in ferromagnetic thin films

T. C. Chuang, P. L. Su, P. H. Wu, and S. Y. Huang*
Department of Physics, National Taiwan University, Taipei 10617, Taiwan
(Received 16 August 2017; revised manuscript received 17 October 2017; published 7 November 2017)

The anomalous Nernst effect (ANE) is one of the most important mechanisms to explore the anomalous Hall heat current in ferromagnets. In this work, we studied the ANE in various ferromagnetic materials with in-plane anisotropy. Surprisingly, we show that the thickness dependence of the ANE on the magnitude and sign is nontrivial, even in conventional ferromagnetic metals (FMs), including Fe, Co, Ni, and Py ($Ni_{80}Fe_{20}$). While the sign of the ANE of Fe is opposite to that of Co, Ni, and Py in thicker films, it can even be reversed via decreasing thickness. Most importantly, the anomalous Nernst angles θ_{ANE} for these FMs show a unified behavior. They can be significantly enhanced by up to one order of magnitude in ultrathin films. By systematically studying the thickness dependence of the electrical and thermal transport properties, we show that the enhanced ANE of FMs is dominated by spin-orbit coupling through the intrinsic and side-jump mechanisms.

DOI: 10.1103/PhysRevB.96.174406

I. INTRODUCTION

The spin Seebeck effect (SSE) and the anomalous Nernst effect (ANE) have played a significant role in spin caloritronics [1,2]. As the relativistic spin-orbit coupling phenomena can be explored through the interaction between charge, spin, and heat, the SSE and ANE have attracted a great deal of attention regarding the generation of pure spin current and spin-polarized current by a thermal gradient. Furthermore, the spin-dependent thermal voltage generated by the SSE and ANE offers an alternative approach to exploiting novel thermoelectric devices, which might overcome the restriction of the Wiedemann-Franz law [2]. Although the thermal-energy conversion efficiency is still small, recent works show that the superposition of the SSE and ANE in thin films could dramatically enhance the transverse thermopower in the lateral thermopile [3–5] or multilayer structure [5–8]. Moreover, a large ANE was just reported in a noncollinear antiferromagnet Mn_3Sn, despite negligibly small magnetization [9,10]. These intensive studies on the interplay between thermoelectric transport and spin configurations have shed light on spin caloritronics and its applications.

For thin films, it is known that the thickness of a spin current detector should be comparable to its spin-diffusion length, typically 1–10 nm; otherwise the SSE signal could be significantly reduced [11,12]. However, the behavior of the thickness-dependent ANE remains poorly known [13,14]. The ANE is the thermal counterpart of the anomalous Hall effect (AHE) [15] as shown in Fig. 1(a). When a temperature gradient ∇T or an electric gradient ∇V is applied to a ferromagnetic metal (FM), the electric field $\boldsymbol{E}$ emerges along the direction perpendicular to both the magnetization and the applied ∇T or ∇V by the ANE or AHE, respectively. Since the ANE (AHE) in the FM metal and the spin Hall effect (SHE) in the nonmagnetic metal both involve the separation of charge carriers with opposite spins, they share the same origin of spin-orbit coupling [16]. Consequently, the spin-dependent voltage induced by the ANE (AHE) in various FMs and that induced by the SHE in nonmagnetic metals can be of either sign. While the sign of the SHE is based on the number of electrons on d orbitals [17], there is no simple rule to determine the sign of ANE or AHE in FMs.

In this work, we experimentally demonstrate that the thickness dependence of the ANE signal, not just for the magnitude but also for the sign, is nontrivial, even in conventional ferromagnetic materials (FMs), including Fe, Co, Ni, and Py ($Ni_{80}Fe_{20}$). We show that the sign of the ANE of Fe is opposite to that of Co, Ni, and Py in thicker films and can be reversed via decreasing the thickness. The anomalous Nernst angle θ_{ANE} and the conversion efficiency of the spin/charge signal generated by heat flows, can all be significantly enhanced in ultrathin films. After systematically studying the thickness dependence of electrical and thermal transport properties, we demonstrate that the enhanced θ_{ANE} of Py is dominated by skew scattering and that of Fe, Co, and Ni is due to the intrinsic and side-jump mechanisms. Furthermore, the enhancement of the ANE in thin ferromagnetic films is strikingly dominant in the multilayer system.

II. MATERIAL GROWTH, CHARACTERIZATION, AND EXPERIMENTAL CONFIGURATION

The FMs films, including Fe, Co, Ni, and Py, are grown on Si or glass substrates by magnetron sputtering at room temperature. To prevent films from oxidation, a 5-nm MgO capping layer is deposited by rf magnetron sputtering. Atomic force microscopy (AFM) is used to measure their thickness and surface roughness. The resistivity is measured by the four-probe method. The magnetic properties, including the magnetization ($\boldsymbol{M}$) and magnetic hysteresis loops, are investigated with vibrating sample magnetometer (VSM). To generate a thermally spin-polarized current by the ANE, we employ the longitudinal experimental setup with a uniform out-of-plane temperature gradient (∇T_z), as shown in Fig. 1(b) [18,19]. The temperature gradient is measured with thermocouples. To reduce systematic errors, we use a constant power with the same heat flux density instead of a constant temperature difference to conduct the measurement [20–22]. An external in-plane magnetic field ($\boldsymbol{H}$) is used to align the magnetization of all FMs. Note that the measurement resolution of thermal voltage is less than 0.05 μV, which is much smaller than the data symbol size.

*syhuang@phys.ntu.edu.tw

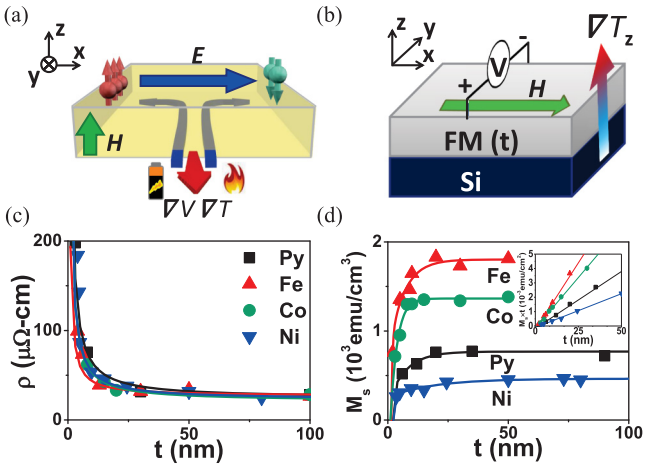

FIG. 1. (a) Schematic diagrams of the anomalous Nernst effect (ANE) with a thermal gradient ∇T and the anomalous Hall effect (AHE) with an electric field gradient ∇V. The electric field $\boldsymbol{E}$ emerges along the x direction perpendicular to both the magnetic field (H) in the z direction and the applied ∇T or ∇V in the y direction by the ANE or AHE, respectively. (b) Schematic of ANE measurement with the temperature gradient along the z axis (∇T_z) and the magnetization in the x-y plane. (c) Thickness dependence of resistivity (ρ) and (d) thickness dependence of saturation magnetization (M_s) for different ferromagnetic materials, including Fe, Co, Ni, and Py. The sold lines are a fit to the results. The inset in (d) shows the linear fit to the thickness-dependent magnetization.

Figures 1(c) and 1(d) show the electrical resistivity (ρ) and the saturation magnetization for a series of films with different thicknesses (t), including Fe, Co, Ni, and Py. For all FM films, the resistivities are constant in thick layers with values around 26, 20, 22, and 24 $\mu\Omega$ cm, respectively [23–25], and they systematically increase with decreasing thicknesses to a few hundreds of $\mu\Omega$ cm in the thinnest films. The behavior of thickness-dependent resistivity can be well fitted with solid lines by taking into account the surface and grain-boundary scattering within Matthiessen's rule [26]. The saturation magnetization per unit volume (M_s) in thick layers of Fe, Co, Ni, and Py is about 1.7, 1.4, 0.5, and 0.8×10^3 emu/cm^3 respectively, which are all consistent with that of the bulk values. Figure 1(d) shows that M_s decreases with decreasing thickness, because of the finite size effect. They cross zero at the criticalthicknesses, which are 1.4, 1.1, 2.3, and 2.2 nm with an error bar of about ± 0.25 nm for Fe, Co, Ni, and Py, respectively, from the intercept of the linear fitting in the inset of Fig. 1(d). Thin films, whose thicknesses are larger than 20 nm with bulk properties, are considered to be in the bulk region in this study.

III. RESULTS AND DISCUSSION

The spin-polarized current can be detected as an electromotive force $\boldsymbol{E}$ by means of the ANE in FMs, and can be described by the following formulas [27],

$$\boldsymbol{E} = -Q_s 4\pi \boldsymbol{M_s} \times \nabla T \quad (1)$$

$$= -S_{xy}\boldsymbol{m} \times \nabla T \quad (2)$$

$$= \theta_{ANE} S_{xx} \boldsymbol{m} \times \nabla T, \quad (3)$$

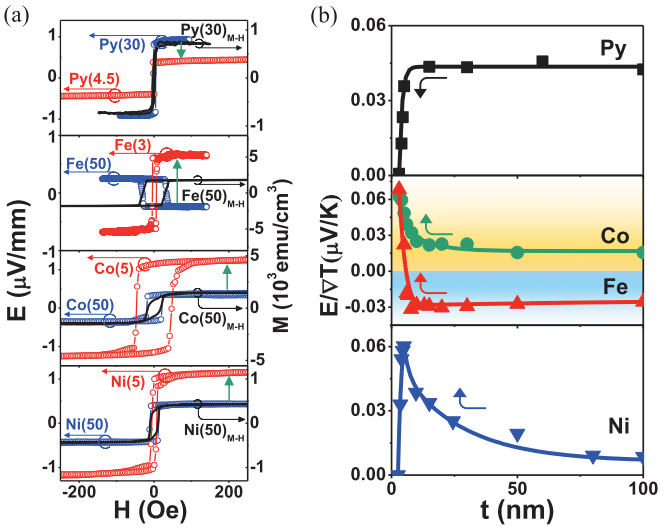

FIG. 2. (a) Anomalous Nernst signal of Fe, Co, Ni, and Py (left y axis) as a function of magnetic field for the thicker and thinner films and magnetic hysteresis loop of Fe, Co, Ni, and Py measured by VSM (right y axis and solid black curves) for a thicker film. (b) Normalized anomalous Nernst signal as a function of thickness of Fe, Co, Ni, and Py.

where Q_s is the ANE coefficient, S_{xy} is the transverse Seebeck coefficient, $\boldsymbol{m}$ is the unit vector of the magnetic moment, S_{xx} is the longitudinal Seebeck coefficient, and θ_{ANE} is the anomalous Nernst angle. In addition, according to Ohm's law, the electric field should also be proportional to the product of current density and resistivity. Since the electrical and magnetic properties are both thickness dependent, the property of thermal transport should be affected accordingly but may have been overlooked previously.

In Fig. 2(a), we show the signal of the ANE, normalized by the distance between the electrical contacts, as a function of the in-plane magnetic field. For FM films with the same thicknesses, the hysteresis loop of ANE (blue open circle) follows that of the magnetization (solid black curve) as described in Eq. (1). However, what is more complicated is the sign of the ANE signal. In the bulk region with thicker films, where the sign of the ANE of Fe (50) is opposite to that of Py (30), Co (50), and Ni (50), the sign of Fe can be surprisingly reversed when we compare the signal between 50- and 3-nm Fe. Even more interesting is that the magnitude of the ANE signal can be enhanced in thinner films of Fe, Co, and Ni, but reduced in Py. Such dramatically different behavior can only be clearly revealed as one studies the thickness dependence behavior of the ANE, as shown in Fig. 2(b). Here, the data points for the ANE signal are taken when the magnetization is saturated at 200 Oe. The thermal signal induced by the ANE is systematically enhanced with decreasing thickness of Co and Fe, but the trend is opposite to that of Py, which decreased with decreasing thicknesses. In the case of Ni, the ANE signal increases with decreasing thickness and has a sharp drop at 5 nm. Note that the sign of the ANE of Fe is not always negative, and it can be further reversed when the thickness is thinner than 6 nm. Although the thickness-dependent behaviors varied with materials, the

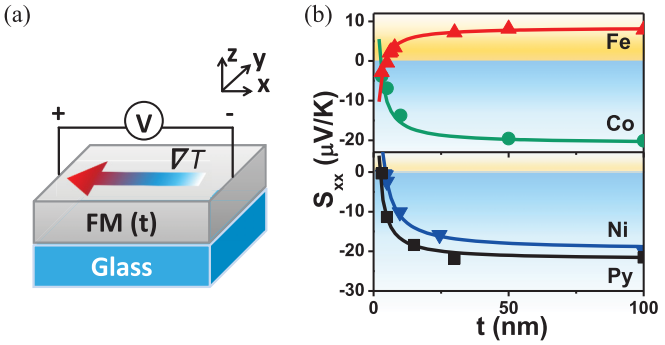

FIG. 3. (a) Schematic diagrams of the longitudinal Seebeck coefficient S_{xx} measurement. The temperature gradient (∇T) is applied along the x direction and the thermal voltage (V) is measured in the same direction. (b) Thickness dependence of S_{xx} for Fe, Co, Ni, and Py. Solid lines show fit curves obtained by using the effective mean free path model.

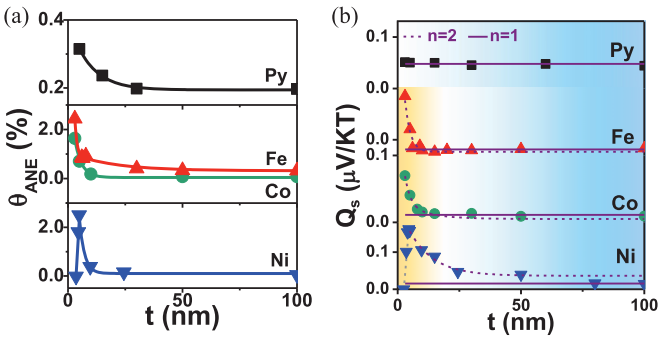

FIG. 4. (a) Anomalous Nernst angle as a function of thickness of Fe, Co, Ni, and Py. (b) Thickness dependence of the anomalous Nernst coefficients Q_s for Fe, Co, Ni, and Py. Dashed lines and solid lines show best-fit curves obtained by using $n = 2$ (yellow area) and $n = 1$ (blue area) in Eq. (5), respectively.

ANE for FMs with thicknesses thinner than 2 nm are all too small to be measured. This threshold thickness corresponds to the critical thickness of M_s and is caused by the finite size effect.

The striking thickness dependence of ANE for the four conventional FMs in Fig. 2(b) is clearly not following the rising resistivity due to surface scattering in Fig. 1(c) or the magnetization reduction due to the finite size effect in Fig. 1(d). The thickness dependence of ANE in FMs has been overlooked. According to Eq. (3), the ANE is also strongly related to the Seebeck coefficient. As we have previously demonstrated that the Seebeck coefficient between bulk and film could be different, such as in a Pt wire and Pt film [19], it is important to investigate the thickness dependence of the Seebeck effect. The Seebeck coefficient S_{xx} is described by the Mott formula, $S_{xx} = \frac{\pi^2 k_B^2 T}{3e\sigma}(\frac{\partial\sigma}{\partial E})_{E_F}$ [28,29]. Here k_B is the Boltzmann constant, e is the electric charge, σ is the electrical conductivity, and E_F is the Fermi energy. Since S_{xx} depends on the derivative of the electrical conductivity at the Fermi level, when the film thickness is comparable to or less than the carrier mean free path, S_{xx} could be significantly influenced by surface scattering. To measure the longitudinal Seebeck coefficient S_{xx}, we apply an in-plane temperature gradient to the ferromagnetic samples with different thicknesses on insulating glass substrates, as illustrated in Fig. 3(a). The experimental results of the thickness-dependent S_{xx} for different FMs in Fig. 3(b) shows that S_{xx} of Fe, Co, Ni, and Py are saturated at 9, -21, -20, and -22μV/K, respectively, when the thicknesses are in the bulk region. The absolute values of S_{xx} for FMs all decrease with decreasing thickness. This behavior can be described by the mean free path model $S_{xx}(t) = S_g(1 - b/t)$ [19,30], as the solid lines shown in Fig. 3(b). Here S_g is the bulk Seebeck coefficient, b is the parameter related to surface and grain-boundary scattering, and t is the thickness of the film. Therefore, the S_{xx} could change its sign when the film thickness is thin enough owing to significant scattering. In the case of Fe, the sign change of S_{xx} occurs at around 6 nm, which is consistent with that of the ANE signal for Fe films in Fig. 2(b). Unlike the electrical transport where the sign of the voltage is determined with given current direction, the Seebeck voltage in the thermal transport can have either sign under a fixed temperature gradient. The magnitude and the sign of the Seebeck coefficient are thickness dependent. Our results highlight that the sign of the ANE signal depends on both the Seebeck coefficient and the anomalous Nernst angle.

By combining Eqs. (2) and (3), we can experimentally derive the thickness-dependent θ_{ANE} in Fig. 4(a). The values of θ_{ANE} for FMs in the bulk region are all around 0.1%–0.2%, which are similar to that of the anomalous Hall angle θ_{AHE}, but the signs of θ_{ANE} are all positive, unlike θ_{AHE} which can be of either sign. Most importantly, the θ_{ANE} of all four FMs can be significantly enhanced by decreasing the thickness. Especially for Fe, Co, and Ni, the θ_{ANE} enhancement can be more than 10 times for thin films comparing with bulk.

The origin of the ANE is spin-orbit interaction, which can be decomposed into the intrinsic Berry curvature, the side jump, and the skew scattering mechanism, which is analogous to the AHE. To investigate the scaling relation of the ANE, we use the equation of the transverse Seebeck coefficient, S_{xy},

$$S_{xy} = \rho(\alpha_{xy} - S_{xx}\sigma_{xy}). \tag{4}$$

where the transverse thermal conductivity α_{xy} can be derived from the Mott relation as $\alpha_{xy} = \frac{\pi^2 k_B^2 T}{3e}(\frac{\partial\sigma_{xy}}{\partial E})_{E_F}$ [31,32], the transverse electrical conductivity σ_{xy} can be substituted by the power-law scaling of $\rho_{xy} = \lambda M \rho^n$, and λ represents the strength of the spin-orbit coupling [32]. As a result, we obtain the following relation from Eqs. (1), (2), and (4):

$$\frac{Q_s}{\rho^{n-1}} = \frac{\pi^2 k_B^2 T}{3e}\lambda' - (n-1)\lambda S_{xx}. \tag{5}$$

According to the power-law scaling, skew scattering requires $n = 1$, while the intrinsic and side-jump mechanisms have $n = 2$. To determine the exponent n in our experiment, we plot Q_s as a function of thickness by taking into account the experimental results of the $S_{xx}(t)$ and $\rho(t)$ in Fig. 4(b). In the thin-film region ($t < 20$ nm), the best-fit value of n for Fe, Co, and Ni is 2 which is represented by the dashed lines; therefore, the intrinsic and side-jump contributions are the dominant mechanisms for the ANE enhancement. On the other hand, the second term in Eq. (5) vanishes if $n = 1$, indicating that

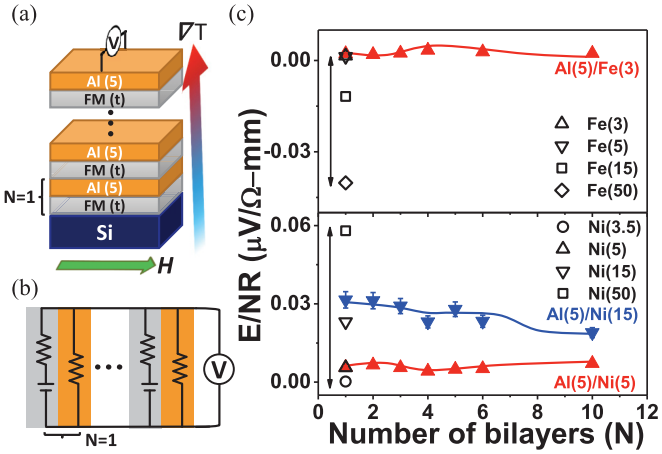

FIG. 5. (a) Schematic diagrams of the ANE measurement for $[Al(5)/FM(t)]_N$ multilayer structure. (b) Schematic diagrams of parallel circuit model for multilayer structure with PM and FM layers. (c) Normalized anomalous Nernst signal in multilayer as a function of number of bilayers N for $[Al(5)/Fe(3)]_N$ in the top panel and $[Al(5)/Ni(3)]_N$ and $[Al(5)/Ni(3)]_N$ in the bottom panel. Open symbols represent a single Fe (top) and Ni (bottom) layer with different thicknesses.

the ANE signal is independent of S_{xx} and the thickness. The constant behavior in Fig. 4(b) for Py and for Co, Fe, and Ni in the thick-film region suggests that the extrinsic skew scattering gives the leading contribution, as shown with solid lines. Thus the contribution from the power-law $n = 2$ scatterings (intrinsic and side jump) gradually decay by increasing the thickness. Our results are consistent with the Mott relation and show that the ANE excited by heat current is very sensitive to the details of the electronic band structure. Furthermore, reducing the film thicknesses, not only by impurity scattering, but also by the intrinsic contribution from the modification of band structure may lead to the enhancement of the ANE as demonstrated in our results.

Recently, the paramagnet (PM)/ferrimagnet or PM/FM multilayers have attracted great attention due to the enhanced thermal voltages induced by the superposition of the longitudinal spin Seebeck effect (SSE) and the ANE [5–8]. Such a multilayer system can be viewed as several independent bilayers (PM/FM) electrically connected in parallel, as shown in Fig. 5(b). However, the effect of thickness on the thermal voltage has never been considered. In one report, the enhancement of the thermal voltage is even observed in the Cu/FM multilayer system with constant total thickness but increased multilayer number [7]. Since the nonmagnetic metal Cu has negligible spin-orbit coupling, the enhancement is not expected and should not originate from the longitudinal SSE or the ANE. While the enhancement mechanism is not yet clear, our results of thickness-dependent ANE may provide some insights.

To investigate the contribution of the thickness-dependent ANE in multilayers, a series of $[PM/FMs]_N$ samples are fabricated and the thermal voltage is measured under a vertical temperature gradient, as illustrated in Fig. 5(a). To clarify the origin of the enhanced thermal signal in multilayers, we use a small atomic number element, Al, with negligible spin-orbit coupling as the PM layer. According to the parallel circuit model in Fig. 5(b), we normalize the thermal signal in Fig. 5(c) by sheet resistance and N to obtain the individual PM/FM bilayer's contribution. For comparison, the values of the ANE for the single-layer Fe and Ni with different thicknesses are also included. It is clear that the dependence of the thermal signal for $[Al(5)/Fe(3)]_N$, $[Al(5)/Ni(5)]_N$, and $[Al(5)/Ni(15)]_N$ on N is not strong. However, the ANE can significantly be enhanced by one order of magnitude when the thickness of Fe or Ni is changed. The results conclusively demonstrate that the thickness dependence of the ANE, especially for thin films, plays an important role in enhancing the spin-current-driven thermoelectric signal.

IV. CONCLUSION

In summary, we have investigated the thickness dependence of the ANE in several conventional ferromagnetic metals, including Fe, Co, Ni, and Py. The sign and magnitude of the ANE show different behaviors against the thickness of different ferromagnetic materials. By studying the thickness dependence of S_{xx}, we find that θ_{ANE}'s are significantly enhanced with decreasing thickness for all ferromagnetic materials as a unified behavior. According to the Mott relation, the ANE can be paraphrased by a power-law relation between the anomalous Nernst coefficient and the longitudinal resistivity. We show that the enhancement in thin films is largely caused by the intrinsic and side-jump mechanisms. Our results highlight that the spin-polarized current excited by the ANE, which is strongly correlated with the band structure and the Berry curvature around the Fermi level, could be dramatically changed in an ultrathin film and will lead to various spin-based thermoelectric applications in spin caloritronics.

ACKNOWLEDGMENTS

We thank D. Qu from the University of Tokyo and L. K. Achaiah from National Taiwan University for fruitful discussion. This work was supported by the Ministry of Science and Technology of Taiwan, under Grants No. MOST 103-2212-M-002-021-MY3 and No. MOST 106-2628-M-002-015-MY3. S.Y.H. acknowledges the support of the Golden Jade Fellowship of the Kenda Foundation, Taiwan.

[1] G. E. Bauer, E. Saitoh, and B. J. van Wees, Nat. Mater. **11**, 391 (2012).

[2] K. I. Uchida, H. Adachi, T. Kikkawa, A. Kirihara, M. Ishida, S. Yorozu, S. Maekawa, and E. Saitoh, Proc. IEEE **104**, 1946 (2016).

[3] K. I. Uchida, T. Nonaka, T. Yoshino, T. Kikkawa, D. Kikuchi, and E. Saitoh, Appl. Phys. Express **5**, 093001 (2012).

[4] Y. Sakuraba, K. Hasegawa, M. Mizuguchi, T. Kubota, S. Mizukami, T. Miyazaki, and K. Takanashi, Appl. Phys. Express **6**, 033003 (2013).

[5] R. Ramos, A. Anadón, I. Lucas, K. Uchida, P. A. Algarabel, L. Morellón, M. H. Aguirre, E. Saitoh, and M. R. Ibarra, APL Mater. **4**, 104802 (2016).
[6] R. Ramos, T. Kikkawa, M. H. Aguirre, I. Lucas, A. Anadón, T. Oyake, K. Uchida, H. Adachi, J. Shiomi, P. A. Algarabel *et al.*, Phys. Rev. B **92**, 220407(R) (2015).
[7] K.-i. Uchida, T. Kikkawa, T. Seki, T. Oyake, J. Shiomi, Z. Qiu, K. Takanashi, and E. Saitoh, Phys. Rev. B **92**, 094414 (2015).
[8] K. D. Lee *et al.*, Sci. Rep. **5**, 10249 (2015).
[9] M. Ikhlas, T. Tomita, T. Koretsune, M.-T. Suzuki, D. Nishio-Hamane, R. Arita, Y. Otani, and S. Nakatsuji, Nat. Phys. **10**, 1 (2017).
[10] X. Li, L. Xu, L. Ding, J. Wang, M. Shen, X. Lu, Z. Zhu, and K. Behnia, Phys. Rev. Lett. **119**, 056601 (2017).
[11] D. Qu, S. Y. Huang, B. F. Miao, S. X. Huang, and C. L. Chien, Phys. Rev. B **89**, 140407(R) (2014).
[12] D. Qu, S. Y. Huang, and C. L. Chien, Phys. Rev. B **92**, 020418(R) (2015).
[13] S. Y. Huang, X. Fan, D. Qu, Y. P. Chen, W. G. Wang, J. Wu, T. Y. Chen, J. Q. Xiao, and C. L. Chien, Phys. Rev. Lett. **109**, 107204 (2012).
[14] H. Kannan, X. Fan, H. Celik, X. Han, and J. Q. Xiao, Sci. Rep. **7**, 6175 (2017).
[15] N. Nagaosa, J. Sinova, S. Onoda, A. H. MacDonald, and N. P. Ong, Rev. Mod. Phys. **82**, 1539 (2010).
[16] J. Sinova, S. O. Valenzuela, J. Wunderlich, C. H. Back, and T. Jungwirth, Rev. Mod. Phys. **87**, 1213 (2015).
[17] T. Tanaka, H. Kontani, M. Naito, T. Naito, D. S. Hirashima, K. Yamada, and J. Inoue, Phys. Rev. B **77**, 165117 (2008).
[18] P. H. Wu and S. Y. Huang, Phys. Rev. B **94**, 024405 (2016).
[19] Y. J. Chen and S. Y. Huang, Phys. Rev. Lett. **117**, 247201 (2016).
[20] A. Sola, P. Bougiatioti, M. Kuepferling, D. Meier, G. Reiss, M. Pasquale, T. Kuschel, and V. Basso, Sci. Rep. **7**, 46752 (2017).
[21] B. W. Wu, G. Y. Luo, J. G. Lin, and S. Y. Huang, Phys. Rev. B **96**, 060402(R) (2017).
[22] F. J. Chang, J. G. Lin, and S. Y. Huang, Phys. Rev. Mater. **1**, 031401(R) (2017).
[23] T. Miyasato, N. Abe, T. Fujii, A. Asamitsu, S. Onoda, Y. Onose, N. Nagaosa, and Y. Tokura, Phys. Rev. Lett. **99**, 086602 (2007).
[24] S. J. Watzman, R. A. Duine, Y. Tserkovnyak, S. R. Boona, H. Jin, A. Prakash, Y. Zheng, and J. P. Heremans, Phys. Rev. B **94**, 144407 (2016).
[25] Y. Q. Zhang, N. Y. Sun, R. Shan, J. W. Zhang, S. M. Zhou, Z. Shi, and G. Y. Guo, J. Appl. Phys. **114**, 163714 (2013).
[26] L. I. Maissel and R. Glang, *Handbook of Thin Film Technology* (McGraw-Hill, New York, 1970).
[27] K. Hasegawa, M. Mizuguchi, Y. Sakuraba, T. Kamada, T. Kojima, T. Kubota, S. Mizukami, T. Miyazaki, and K. L. Takanashi, Appl. Phys. Lett. **106**, 252405 (2015).
[28] S. Y. Huang, W. G. Wang, S. F. Lee, J. Kwo, and C. L. Chien, Phys. Rev. Lett. **107**, 216604 (2011).
[29] M. Cutler and N. F. Mott, Phys. Rev. **181**, 1336 (1969).
[30] C. R. Pichard, C. R. Tellier, and A. J. Tosser, J. Phys. F: Met. Phys. **10**, 2009 (1980).
[31] G. Y. Guo, Q. Niu, and N. Nagaosa, Phys. Rev. B **89**, 214406 (2014).
[32] Y. Pu, D. Chiba, F. Matsukura, H. Ohno, and J. Shi, Phys. Rev. Lett. **101**, 117208 (2008).